CrossMark

ORIGINAL PAPER

Assessing the potential origins and human health risks of trace elements in groundwater: A case study in the Khoy plain, Iran

Rahim Barzegar · Asghar Asghari Moghaddam · Jan Adamowski · Amir Hossein Nazemi

Abstract The objectives of this study were to measure some trace element concentrations in the groundwater of the Khoy area in northwestern Iran, understand their potential origins using multivariate statistical approaches (correlation analysis, cluster analysis and factor analysis), and evaluate their non-carcinogenic human health risks to local residents through drinking water intake. The trace element status of the groundwater and the associated health risks in the study area have not previously been reported. Groundwater water samples were collected from 54 water sources in July 2017 in the study area. Samples were measured for EC, pH, major and minor elements and some trace elements (Fe, Mn, Al, Zn, Cr, Pb, Cd, Co, Ni and As). The levels of EC, F, Cd, Pb, Zn, As and all the major ions except K exceeded permissible levels for drinking water. Multivariate analysis showed that the quality of groundwater was mainly controlled by geogenic factors followed by anthropogenic impacts. Health risk assessment results indicated that Cr and As in the groundwater, with hazard quotient values of 0.0001 and 11.55, respectively, had the lowest and highest impacts of non-carcinogenic risk to adults and children in the area. The high-risk samples were mainly situated in the northeast and southwest of the Khoy plain where the groundwater was saline. The health risk associated with water consumption from the unconfined aquifer was higher than that from the confined aquifer in the study area. Special attention should be paid to groundwater management in the high-risk areas to control factors (e.g., EC, pH and redox) that stimulate the release of trace elements into groundwater.

R. Barzegar (✉) · A. Asghari Moghaddam
Department of Earth Sciences, Faculty of Natural Sciences, University of Tabriz, 29 Bahman Boulevard, Tabriz, Iran
e-mail: rm.barzegar@yahoo.com;
rahim.barzegar@mail.mcgill.com

R. Barzegar · J. Adamowski
Department of Bioresource Engineering, McGill University, 21111 Lakeshore, Ste Anne de Bellevue, Quebec H9X3V9, Canada

A. H. Nazemi
Department of Water Engineering, Faculty of Agriculture, University of Tabriz, 29 Bahman Boulevard, Tabriz, Iran

Introduction

In recent decades, industrial and population growth have led to increased demand worldwide for freshwater resources, especially groundwater. The over-exploitation of groundwater along with contamination caused by human activities has put freshwater supplies at risk (Li et al. 2017). Trace elements are among the most hazardous contaminants of water due to their

distinct characteristics including chemical stability, weak degradation, wide range of sources, serious toxicity, bioaccumulation and difficulties in remediation (Li et al. 2015; Sun et al. 2016), and they can pose significant threats to humans and the environment. Some trace metals are essential nutrients at low levels but can lead to severe poisoning at higher concentrations. Trace element contamination mainly originates from natural (weathering and dissolution of rocks) and anthropogenic (mining, industrial and agricultural) processes and activities that can deteriorate the quality of water for drinking, agricultural and industrial purposes (Barzegar et al. 2017).

Knowledge of potential sources of trace elements and their content in groundwater is important for sustainable and effective management of groundwater resources. The potential origin of trace elements in a groundwater system can be determined by graphical and multivariate statistical methods and modeling approaches (e.g., diffusion and receptor models, Sun et al. (2016)). Multivariate methods are increasingly being used because of their easy application and ability to compare large amounts of information, which is very difficult to do using number tables or univariate statistics (Bingöl et al. 2013). Among the multivariate approaches, correlation analysis, cluster analysis (CA) and factor analysis (FA) are the most widely used statistical methods to determine the source of groundwater quality degradation (Yidana et al. 2010; Purushothaman et al. 2014; Wu et al. 2014; Barzegar et al. 2017, 2018 and Soltani et al. 2017). Correlation analysis deciphers the relationships between hydrochemical variables to identify their potential origins. CA reveals similarities between samples and groups of samples. FA does not require prior knowledge of the number of sources and source characteristics of the contaminants, and is used to determine the potential hydrogeochemical processes and effective factors (e.g., natural and anthropogenic) in groundwater quality. Many studies to identify the origins of trace elements in groundwater by multivariate statistics have been carried out in different parts of the world (Li et al. 2014; Purushothaman et al. 2014; Esmaeili et al. 2018; Barzegar et al. 2017, 2018). These studies showed that multivariate approaches were able to discover the potential origins of contaminants in water as well as hydrogeochemical processes. For instance, Barzegar et al. (2018) investigated the potential source of some selected trace elements in

groundwater of the Shabestar area, northwestern Iran, using multivariate statistical analysis. The outcomes indicated that weathering and dissolution of rocks, particularly silicates and evaporites, ion exchange processes, water salinity, and alkalinity were the main factors resulting in the release of trace elements into the groundwater of the area. The impacts of nitrate along with zinc in fertilizers and agrochemicals were responsible for 10% of the total variance in groundwater quality. Esmaeili et al. (2018) evaluated the potential origins of trace elements including iron (Fe), manganese (Mn), zinc (Zn), chromium (Cr), lead (Pb), cadmium (Cd), aluminum (Al) and arsenic (As) utilizing correlation coefficient, CA and FA analyses in groundwater of the Qareh-Ziaeddin area, in northwestern Iran. They inferred that weathering and dissolution of evaporitic formations, igneous rocks with fluoride-bearing minerals and serpentinite rocks, denitrification and cation exchange, were the prevailing processes in the groundwater of the study area. Moreover, FA confirmed the geogenic impacts with a total variance of 83% on the groundwater quality.

Exposure to potentially toxic chemicals such as trace elements in water can cause serious adverse human health effects, including a variety of cancers, intellectual disabilities, and neurological, cardiovascular, kidney and bone diseases (Adriano 2001; Järup 2003; Li and Qian 2011; Prüss-Ustün et al. 2011). Potential exposure to a mixture of trace elements can be evaluated by a health risk assessment, which is used to understand the potential of a risk source to introduce risk agents into the environment, to estimate the quantity of risk agents that come into contact with human–environment boundaries, and to quantify the health consequences of exposure (Ma et al. 2007; Giri and Singh 2015). Many researchers (e.g., Nguyen et al. 2009; Rahman et al. 2009; Wongsasuluk et al. 2014; Celebi et al. 2014; Li et al. 2014; Liang et al. 2016; Barzegar et al. 2018) have reported on the human health risks of trace elements in groundwater. For example, Liang et al. (2016) evaluated the health risk of As pollution in drinking groundwater in southern Taiwan based on the hazard quotient (HQ) and target risk (TR). Results showed that the HQ values for the 95th percentile were above the value of 1, and TR levels exceeded the threshold value of 10E−6. They concluded that 0.01–7.50% of the population's HQ levels were higher than 1 and 77.7–93.3% of the population was in the high cancer risk category and

had a TR value of 10E−6. The TR calculation outcomes inferred that the use of groundwater for drinking purposes put people at risk of As exposure. Wongsasuluk et al. (2014) investigated the human health risk of heavy metals in drinking water from shallow groundwater wells in an agricultural area in Ubon Ratchathani province, Thailand. According to their results, unacceptable non-carcinogenic health risk levels were detected at some water wells for As, Cu, Zn and Pb with HQs ranging from 0.004 to 2.901, 0.053 to 54.818, 0.003 to 6.399 and 0.007 to 26.80, respectively. The hazard index (HI) values (ranging from 0.10 to 88.21) exceeded allowable limits in 58% of the wells. Although the concentrations of these elements were within acceptable ranges for drinking, As had an unacceptable cancer risk at some water wells, indicating the significance of actual consumption rates in estimating health risk factors.

The Khoy area in Iran's West Azerbaijan province is a fertile and industrialized area. The drinking water in the villages and in the city of Khoy, as well as irrigation of agricultural lands, is very dependent on groundwater. The trace element status of the groundwater and associated health risks in the study area have not previously been reported. Therefore, this study was carried out on the groundwater system of the Khoy area to: (1) identify and measure trace elements including iron (Fe), manganese (Mn), arsenic (As), lead (Pb), cadmium (Cd), cobalt (Co), zinc (Zn), chromium (Cr), aluminum (Al) and nickel (Ni) and determine their potential origins; and (2) evaluate the human health risk of these elements to children and adults through drinking water intake.

## Materials and methods

Study area description

The Khoy plain is located northwest of Urmia Lake, in the northern part of West Azerbaijan province, Iran, and is part of the Aras River drainage basin. The Khoy plain has an area of about 600 km^2 and is bordered by mountains of which the highest is Avrin Mountain (1300 m) in the west of the plain. Surface water resources of the area are mostly two rivers, the Aland and Qotur-Chay, which originate in the western highlands and discharge into the Aras River in the northeast of the plain. Figure 1 shows the location of

the study area including the digital elevation model (DEM) of the Khoy basin and the main rivers. The study area is characterized by a cold arid climate and the annual average rainfall is 292 mm. The 20-year (1997–2017) temperature and humidity averages are 11.6 °C and 60%, respectively. Khoy city is the most important city in the area with more than 348,000 inhabitants. Groundwater is extensively utilized for drinking, agriculture and industrial purposes in the area. The main crops cultivated in the region are sugar cane, sunflower, beets, wheat, barley, corn, lentils, beans, tomatoes, potatoes, chickpeas, alfalfa, melons and watermelons.

Geological and hydrogeological setting

The Khoy area is structurally part of the Khoy-Mahabad sub-zone (the intersection of the Alborz and Sanandaj-Sirjan zones) (Nabavi 1976), which has experienced frequent occurrences of magmatic activity. Magmatic and metamorphic facies, and also recent alluvium, are abundant facies in the area. Figure 2 shows the geological units of the Khoy area. Except for metamorphic rocks with a lithological composition of gneiss, migmatite and schist that are probably related to the Precambrian era, rock units of the Late Precambrian make up the Kahar Formation composed of slate, shale, coal with flakes of graphite, north of Khoy city and are considered the oldest units (Yeganeh et al. 2015). Mesozoic rocks consisting of ophiolitic complex, mafic and ultramafic rocks (e.g., diorite, gabbro, basalt, serpentinite, dunite and harzburgite) and metamorphic rocks (e.g., gneiss, marble, schist related to the Cretaceous period) are found in the western, northern and southwestern parts of the Khoy plain. The Miocene units are made up of conglomerate and represent a disruptive environment. The Upper Miocene to Pliocene deposits, composed of sandstone and conglomerate with marl, shale, layers of gypsum and salt, are known as the Upper Red Formation and can be observed in the west, southeast and northeast of the plain. Units of the Pliocene period are a composition of conglomerate, marl and sandstone, which are distributed in the south and southeast of the plain (Radfar et al. 2005).

Generally, alluvial deposits in the plain resulted from deposition of the Aland and Qotur-Chay Rivers and are mainly composed of gravel, sand and clay. The old terraces are bonded with clay loam, and therefore,
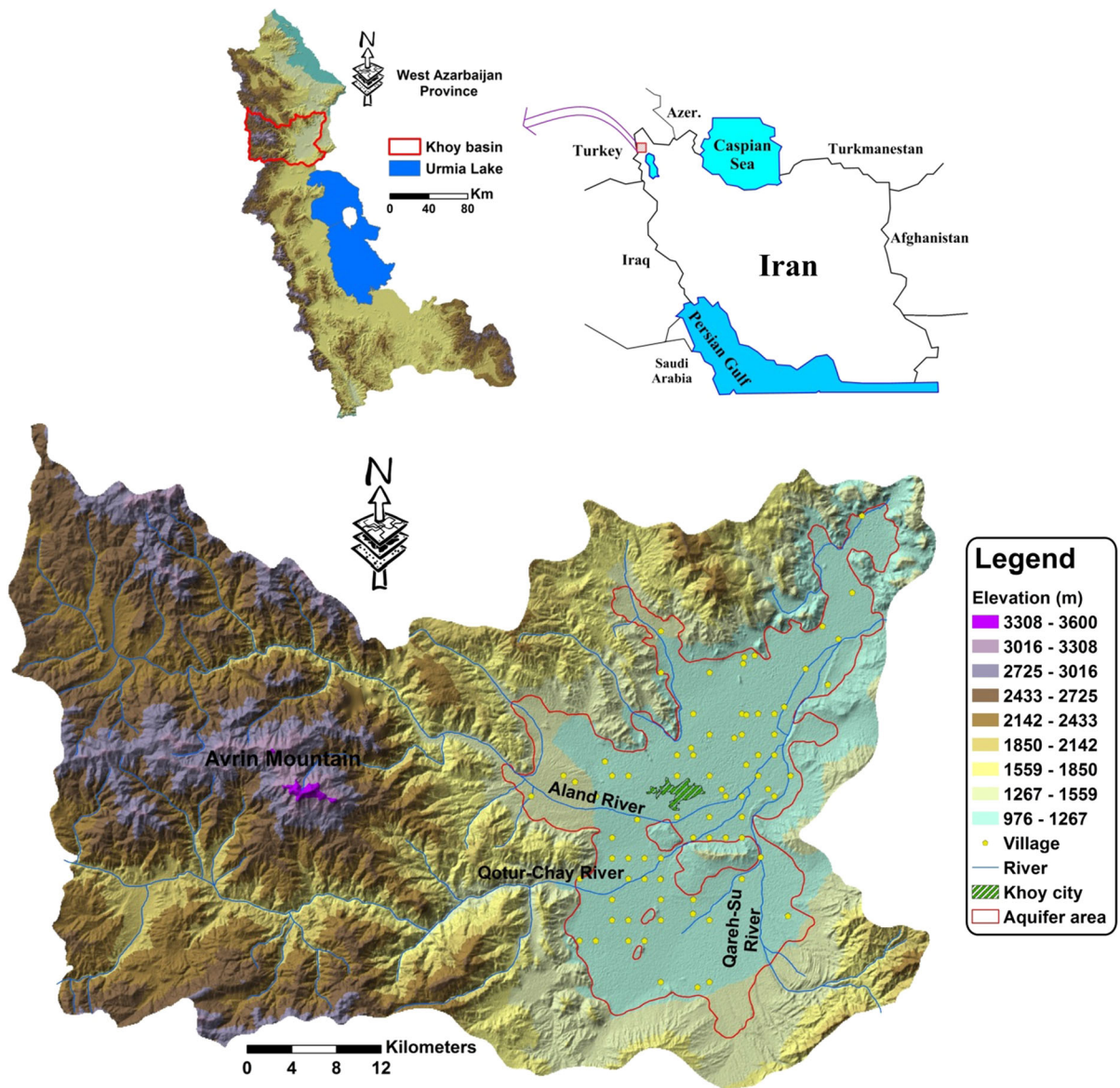
Fig. 1 Digital elevation model (DEM) of the Khoy area and location of the rivers

their permeability is low; recent terraces, located along the rivers, are made of separated sandy grains with high permeability. According to information from geophysical studies, log drillings and geological investigations, the main aquifer was formed in recent alluvial deposits (Quaternary). Aquifers of the Khoy plain consist of two main types: unconfined and confined. Figure 3 shows the schematic position of the aquifers in the plain. The unconfined aquifer covers the entire plain, whereas the confined aquifers are situated in the west and central parts of the plain.

Figure 4 illustrates a geological cross section of the unconfined aquifer in the Khoy plain. Generally, the confined aquifer in the Qotur-Chay River watershed consists of alluvium, which is not uniform in direction of flow and depth. The fine-grained clay and silty layers cause a separation among the deposits, which result in a confined aquifer. In the Aland River watershed, tectonic movement has an important role in the formation of the confined aquifer in the western part of the plain. Displacement of the strata and layers with low permeability on top of coarse-grained layers
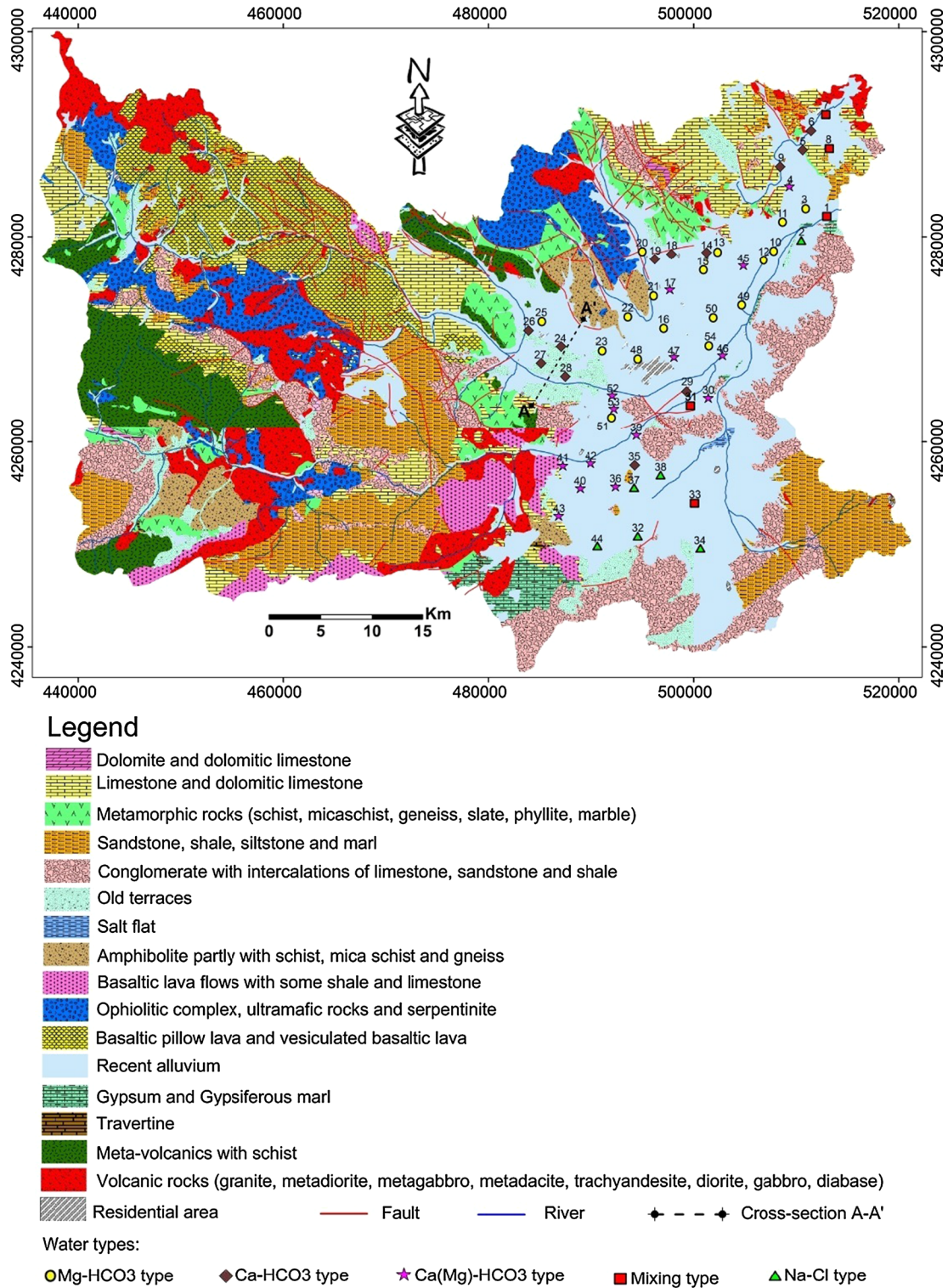
Fig. 2 Geological map of the study area (after Radfar et al. 2005) and location of the sampling sites with water types
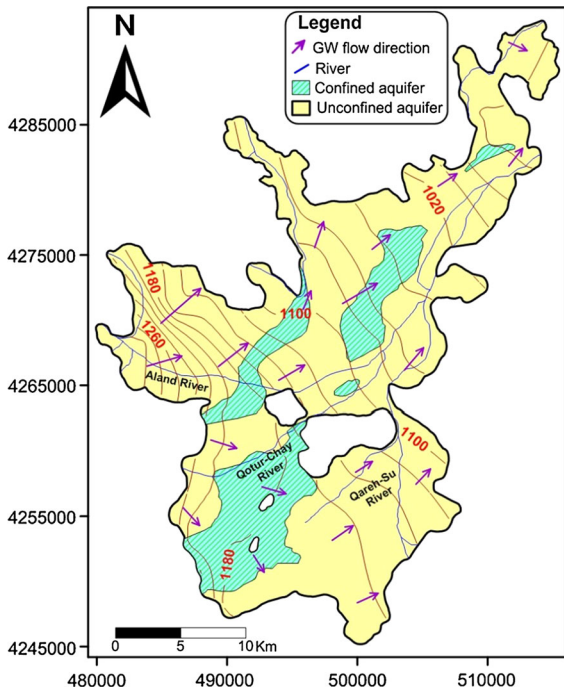
**Fig. 3** Schematic position of the aquifers and unconfined groundwater flow direction in the Khoy plain

by the Firooraq fault resulted in the confined aquifer in the Aland River watershed. Nowadays, due to over-exploitation of groundwater (especially in the north), the confined aquifer has been modified to an

unconfined aquifer hydraulically. Total thickness of the aquifers ranges between 20 and 200 m in the northwest and central part of the plain. The transmissivity values for the unconfined aquifer range between 50 and 1500 m^2/d and pumping tests in the area resulted in an average storage coefficient of 0.05.

The groundwater flow direction is mainly from southwest to northeast. The bedrock of the plain includes marl and conglomerate, which are predominant in the northern and southern parts of the plain, respectively.

Water sampling and analysis

Groundwater water samples were collected from 54 water sources including wells, springs and qanats in July 2017 in the Khoy plain. Figure 2 shows the locations of the sampling points. There are 15 overflow artesian wells in the confined aquifers from which four water samples were collected. Measurements of the pH and electrical conductivity (EC) were recorded in the field using portable instruments, viz. Metrohm 826 and HANNA HI 9033, respectively. Samples were collected in polyethylene bottles, and included one filtered and unacidified sample for major and minor elements, and one filtered and acidified sample for trace element analysis. Acidification and filtration processes were performed using nitric acid
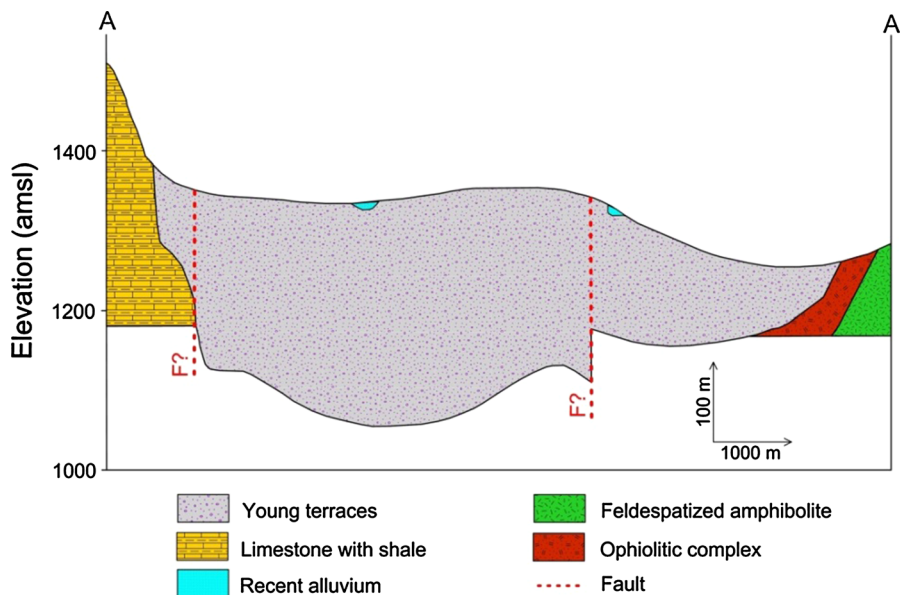
Fig. 4 Geological cross section of the unconfined aquifer in the Khoy plain

and 0.45-µm membrane filters, respectively. Major and minor ions and species were analyzed by titration (for analysis of Ca, Mg, HCO₃ and Cl), flame photometer (for analysis of Na and K) and spectrophotometry (for analysis of SO₄, NO₃, F and SiO₂) according to AHPA (2005) at the Water Laboratory of the University of Tabriz. Accuracy of the chemical analysis of the major ions was checked by computing the cation–anion charge balance (Eq. 1):

$$\text{Charge balance} = \frac{(C - A)}{(C + A)} \times 100, \tag{1}$$

where C and A are the concentrations of total cations (Ca + Mg + Na + K) and total anions (HCO₃ + Cl + SO₄ + NO₃), respectively, in meq/L, and charge balance is the percentage of ionic balance error. The charge balances for all the samples were within the limit of $\pm 5\%$ suggested by Domenico and Schwartz (1998).

Trace elements (Fe, Mn, Al, Zn, Cr, Pb, Cd, Co, Ni and As) were measured using a Varian Spectra 220 Atomic Absorption Spectrometer with GTA 110 at the Water Quality Control Lab of East Azerbaijan Province. Field blank and duplicate procedures were used for quality control assurance. Calibration of equipment was performed linearly with Merck Standard Solutions for each element. The quality control sample was used to check the linearity after every ten samples. Accuracy of the trace element analyses was determined by analyzing certified reference material, NIST SRM. Also, background amendments for all analyses and the nitrous oxide–acetylene flame were used to minimize the risk of interference.

Multivariate statistics

To perform the multivariate statistics, preprocessing (i.e., log transformation and standardization) was employed on the dataset to normalize the measured water quality variables and eliminate the effect of different units of parameters, respectively. For the correlation analysis, a Pearson correlation was applied to decipher the relationships between water quality variables. The strength (r) and significance (p value) of the relationships are two important factors. A larger r indicates a stronger relationship (Barzegar et al. 2016), and in this study, $r > 0.7$, $0.7 > r > 0.5$ and $r < 0.5$ were considered as strong, moderate and weak

relationships, respectively. The smaller the p value, the more significant the relationship (Barzegar et al. 2016).

All measured water quality variables were considered during the hierarchical clustering analysis (HCA) using Ward's method (Ward 1963). This method uses an intra-cluster variation to form clusters, and the clusters are formed by maximizing the homogeneity within each cluster (Hardle and Simar 2007). The squared Euclidean distance is commonly adopted to measure distance or dissimilarity between clusters. The squared Euclidean distance usually expresses the similarity between two samples, and the distance can be shown by the difference between analytical values of the samples (Otto 1998; Bhuiyan et al. 2011; Barzegar et al. 2017).

Factor analysis (FA) is generally employed to recognize the hidden dimension, which may not be explained by direct analysis. The principal component analysis (PCA) is a method to reduce the volume of a large dataset with minimum loss of information (Singh et al. 2017). In total, 19 water quality variables including pH, EC, Ca, Mg, Na, K, HCO₃, SO₄, Cl, NO₃, F, SiO₂, Fe, Mn, Al, Zn, Cr, Pb and As were considered to carry out the FA. The varimax rotation method and Kaiser's criterion (Kaiser 1960) were applied to optimize factor loadings to bring about a simple structure and to extract factors with eigenvalues greater than 1, respectively. Accordingly, factor loadings above 0.75 were considered as high and 0.5–0.75 as medium loadings (Tziritis et al. 2016, 2017). The FA revealed a 0.595 value for the Kaiser–Mayer–Olkin (KMO) and 171 ($p < 0.0001$) for Bartlett's sphericity, indicating that FA was appropriate in providing significant reductions in the dimensionality of the data. The statistical analysis was carried out using SPSS v.21 (IBM Corp 2012).

Human health risk

The non-carcinogenic (chronic) human health risk of trace elements in the groundwater of the Khoy plain was investigated using the method suggested by the U.S. Environmental Protection Agency (USEPA 1999). Chronic daily intake (CDI) of a single trace element through direct ingestion for children and adults was calculated by Eq. 2 (USEPA 1999; Li et al. 2016; Wu and Sun 2016; Zhang et al. 2018):

$$\mathrm{CDI} = \frac{C_\mathrm{W} \times \mathrm{IRW} \times \mathrm{EF} \times \mathrm{ED}}{\mathrm{BW} \times \mathrm{AT}}, \qquad (2)$$

where CDI is exposure dose through intake of groundwater (mg/kg per day), C_w is contaminant concentration in groundwater (mg/L), IRW is the water ingestion rate (L/day, IRW = 2 L/day for adults and 1 L/day for children), EF is exposure frequency (days/year, EF = 365 days/year), ED is exposure duration (years, ED = 70 years for adults and 6 years for children), BW is body weight (kg, BW = 70 kg for adults and 15 kg for children) and AT is average exposure time for non-carcinogens effects (days, AT = 25,550 days for adults and 2190 days for children) (Bortey-Sam et al. 2015; Duggal et al. 2017; Barzegar et al. 2018).

The hazard quotient (HQ) was then calculated by Eq. 3 (Li et al. 2016; Zhang et al. 2018):

$$\mathrm{HQ} = \frac{\mathrm{CDI}}{\mathrm{RfD}}, \qquad (3)$$

where RfD is the reference dose of a specific element (mg/kg per day) and considered as Fe (0.7), Al (1), Cr (1.5), Mn (0.046), As (0.0003), Zn (0.3), Pb (0.0035), Cu (0.04) and Ni (0.02) (mg/kg/day) (Duggal et al. 2017; Barzegar et al. 2018).

The summation of the HQ values of the trace elements gave the hazard index (HI) of each groundwater sample:

$$\mathrm{HI} = \sum \mathrm{HQ}. \qquad (4)$$

The classification of non-carcinogenic human health risk based on USEPA (1999) is presented in Table 1 (Bortey-Sam et al. 2015; Su et al. 2017). HI > 1 indicates that the non-carcinogenic risk of the contaminant exceeds the acceptable limit; HI < 1 demonstrates that the non-carcinogenic risk is within the acceptable limits (USEPA 1999; Li et al. 2016; Su et al. 2017; Zhang et al. 2018).

Results and discussion

Hydrochemistry

Descriptive statistics of the measured water quality parameters are given in Table 2. The pH, with a median value of 7.63, was neutral. EC values ranged between 460 and 7100 µS/cm and were above the permissible level of 1500 µS/cm (WHO 2011) for 40% of the samples. The relative abundance of major and minor cations and anions, based on median values, was found to be Ca > Mg > Na > K and HCO_3 > SO_4 > Cl > NO_3. The order of trace elements content was: Fe > Zn > Al > As > Cr > Pb > Ni > Mn > Co > Cd. The statistical parameters, e.g., skewness and kurtosis, revealed that the majority of the measured parameters, which were outside the range of − 2 to + 2 (Wu et al. 2010; Barzegar et al. 2016), significantly deviated from normality. The levels of EC, F, Pb, Cd, Zn, As and all the major ions except K exceeded the permissible levels for drinking water as recommended by WHO (2011).

A Piper diagram (Piper 1944) was employed to identify water types in the study area (Fig. 5). The majority of samples from the unconfined aquifer and all the samples from the confined aquifers belonged to the Ca(Mg)–HCO_3 water type, characterized by a temporary hardness feature. The spatial distribution of the water types is shown in Fig. 2. Six samples, mainly from the southern part of the plain, showed a saline Na–Cl water type. Samples 1, 7, 8, 31, 33 and 45, mainly from the west of the plain (discharge zone), lay in the E domain of the Piper diagram where none of the cations and anions were predominant. This indicated a mixing zone.

Correlation analysis

The results of the correlation analysis for the groundwater quality variables in the Khoy plain are given in Table 3. There are moderate to strong correlations between EC and major ions including Na ($r = 0.860$, $p < 0.01$), K ($r = 0.838$, $p < 0.01$), HCO_3 ($r = 0.623$, $p < 0.01$), Cl ($r = 0.858$, $p < 0.01$) and SO_4 ($r = 0.820$, $p < 0.01$), which showed the contribution

**Table 1** Classification of non-carcinogenic risk (USEPA 1999)

Risk level	HI	Non-carcinogenic risk
1	< 0.1	Negligible
2	≥ 0.1 < 1	Low
3	≥ 1 < 4	Medium
4	≥ 4	High

Table 2 Descriptive statistics of the measured and analyzed parameters for groundwater samples of the Khoy plain

	Unit	Minimum	Median	Maximum	Std. Dev	Kurtosis	Skewness	WHO (2011)
pH	–	6.53	7.63	8.22	0.43	0.02	− 0.82	6.5–8.5
EC	mg L^{-1}	460.00	1295.00	7100.00	1297.47	4.63	2.00	1500
Ca	mg L^{-1}	16.03	74.47	625.09	124.39	5.94	2.51	200
Mg	mg L^{-1}	22.36	69.98	184.68	34.21	1.84	1.06	50
Na	mg L^{-1}	9.91	59.51	790.98	187.26	4.90	2.40	200
K	mg L^{-1}	0.86	3.69	16.03	3.25	3.64	1.77	12
HCO$_3$	mg L^{-1}	173.24	489.22	1732.40	326.05	2.39	1.49	500
Cl	mg L^{-1}	19.50	79.76	1169.85	286.74	4.70	2.35	250
SO$_4$	mg L^{-1}	0.37	86.23	1534.71	226.35	26.02	4.59	250
NO$_3$	mg L^{-1}	0.25	10.28	43.48	11.69	− 0.14	0.92	50
F	mg L^{-1}	0.00	0.76	1.53	0.28	1.04	0.39	1.5
SiO$_2$	mg L^{-1}	8.32	25.19	170.90	30.87	9.66	2.93	–
Ni	μg L^{-1}	8.00	8.00	17.60	1.94	10.19	3.19	70
Cd	μg L^{-1}	1.00	1.00	4.60	0.80	8.78	2.99	3
Co	μg L^{-1}	3.00	3.00	19.30	4.09	4.95	2.43	–
Pb	μg L^{-1}	2.00	8.25	21.50	4.33	− 0.08	0.50	10
Cr	μg L^{-1}	4.00	10.50	35.20	6.60	2.78	1.58	50
Al	μg L^{-1}	20.00	22.00	132.00	32.44	1.63	1.67	900
Fe	μg L^{-1}	13.20	32.40	1200.00	167.88	36.83	5.69	300
Mn	μg L^{-1}	1.00	4.45	1500.00	280.81	15.13	3.84	400
Zn	μg L^{-1}	0.50	28.37	150.00	24.20	9.27	2.39	50
As	μg L^{-1}	1.00	19.50	52.00	15.98	− 1.04	0.44	10

Fig. 5 Piper diagram of the groundwater samples in the Khoy plain
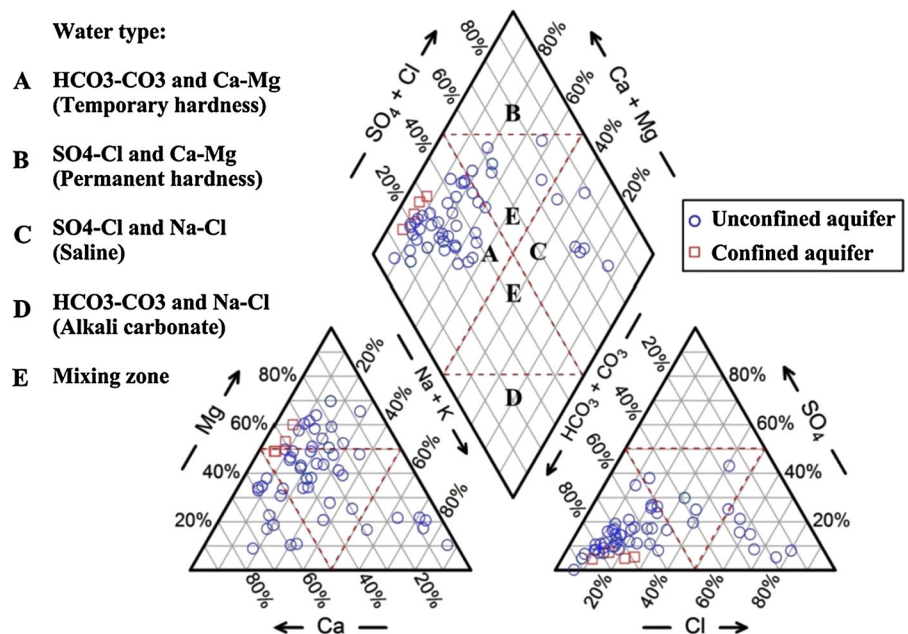
Table 3 Correlation matrix for the water quality parameters in the Khoy plain

	pH	EC	Ca	Mg	Na	K	HCO3	Cl	SO4	NO3	F	SiO2	Ni
pH	1.000												
EC	− 0.493**	1.000											
Ca	− 0.741**	0.666**	1.000										
Mg	− 0.207	0.507**	0.229	1.000									
Na	− 0.120	0.860**	0.238	0.330*	1.000								
K	− 0.314*	0.838**	0.473**	0.441**	0.778**	1.000							
HCO3	− 0.759**	0.623**	0.782**	0.361**	0.261	0.454**	1.000						
Cl	− 0.114	0.858**	0.289*	0.368**	0.951**	0.818**	0.185	1.000					
SO4	− 0.409**	0.820**	0.638**	0.569**	0.621**	0.611**	0.400**	0.640**	1.000				
NO3	− 0.266	0.026	0.126	− 0.258	− 0.013	− 0.272*	0.037	− 0.010	− 0.004	1.000			
F	− 0.486**	0.632**	0.475**	0.261	0.500**	0.545**	0.492**	0.456**	0.557**	0.038	1.000		
SiO2	− 0.382**	0.239	0.238	0.315*	0.066	0.321*	0.559**	0.031	− 0.027	− 0.24	0.390**	1.000	
Ni	− 0.628**	0.575**	0.783**	0.230	0.265	0.468**	0.591**	0.264	0.607**	0.053	0.397**	0.167	1.000
Cd	− 0.359**	0.760**	0.591**	0.355**	0.594**	0.416**	0.428**	0.630**	0.712**	0.313*	0.427**	− 0.024	0.392**
Co	− 0.622**	0.751**	0.823**	0.226	0.463**	0.484**	0.669**	0.500**	0.656**	0.248	0.470**	0.155	0.781**
Pb	− 0.476**	0.493**	0.437**	0.282*	0.304*	0.225	0.404**	0.323*	0.502**	0.258	0.427**	0.112	0.242
Cr	0.090	0.150	0.160	0.175	0.123	− 0.054	0.055	0.093	0.208	0.129	0.17	− 0.032	0.157
Al	− 0.178	0.417**	0.358**	0.318*	0.274*	0.575**	0.313*	0.331*	0.340*	− 0.344*	0.377**	0.394**	0.298*
Fe	− 0.233	0.250	0.365**	0.109	0.091	0.323*	0.493**	0.088	0.012	− 0.233	0.209	0.537**	0.16
Mn	− 0.592**	0.331*	0.526**	0.007	0.129	0.313*	0.633**	0.029	0.159	− 0.003	0.287*	0.342*	0.764**
Zn	− 0.053	0.295*	0.232	0.269*	0.182	0.128	0.327*	0.157	0.247	− 0.010	0.119	0.105	0.16
As	− 0.112	0.353**	− 0.087	0.228	0.500**	0.552**	0.254	0.389**	0.077	− 0.257	0.281*	0.307*	0.08
	Cd	Co	Pb	Cr	Al	Fe	Mn	Zn	As				

pH
EC
Ca
Mg
Na
K
HCO3
Cl
SO4

Table 3 continued

	Cd	Co	Pb	Cr	Al	Fe	Mn	Zn	As
NO$_3$									
F									
SiO$_2$									
Ni									
Cd	1.000								
Co	0.803**	1.000							
Pb	0.536**	0.451**	1.000						
Cr	0.194	0.126	− 0.029	1.000					
Al	0.182	0.249	0.152	0.070	1.000				
Fe	− 0.025	0.122	0.193	− 0.003	0.561**	1.000			
Mn	0.036	0.545**	0.095	− 0.006	0.217	.313*	1.000		
Zn	0.326*	0.313*	0.165	0.211	0.111	0.072	0.043	1.000	
As	0.003	0.078	0.052	− 0.194	0.302*	0.198	0.294*	0.066	1.000

**Correlation is significant at the 0.01 level (two-tailed)

*Correlation is significant at the 0.05 level (two-tailed)

of these ions to the salinity of the groundwater. The negative moderate correlation between pH and EC ($r = -0.493$, $p < 0.01$) indicated the medium effect of acidity on the dissolved content of the water. The pH was also negatively correlated with Ca ($r = -0.741$, $p < 0.01$), HCO$_3$ ($r = -0.759$, $p < 0.01$) and SiO$_2$ ($r = -0.382$, $p < 0.01$), which indicated the effect of HCO$_3$ content on pH and the role of acidity on the dissolution of the silicate minerals. The correlations between pH and Ni ($r = -0.628$, $p < 0.01$), and pH and Co ($r = -0.622$, $p < 0.01$), possibly indicated the role of pH (acidic environment) in releasing these metals into groundwater (Belzile et al. 2004; Balkhair and Ashraf 2016; Barzegar et al. 2016). A strong correlation between Ca and HCO$_3$ ($r = 0.782$, $p < 0.01$) suggested that some of these ions may have been derived from dissolution of calcite. The correlation of Cl with Na ($r = 0.951$, $p < 0.01$), SO$_4$ ($r = 0.640$, $p < 0.01$) and Cl and K ($r = 0.818$, $p < 0.01$) may be attributed to dissolution of halite (NaCl) and sylvite (KCl) minerals and irrigation return flow (Srivastava and Ramanathan 2008). Moderate to high correlations between Ca and Ni ($r = 0.783$, $p < 0.01$), Cd ($r = 0.591$, $p < 0.01$), Co ($r = 0.823$, $p < 0.01$) and Na and Cd ($r = 0.594$, $p < 0.01$) indicated the possible co-enrichment of these metals with the mentioned ions and evaporitic formations as potential sources as suggested by Salminen et al. (2005). The correlation of Na and K ($r = 0.778$, $p < 0.01$) demonstrated the cation exchange process in the groundwater system (El Alfy et al. 2017). A moderate correlation between F and Na ($r = 0.500$, $p < 0.01$) and F and K ($r = 0.545$, $p < 0.01$) might be attributed to the weathering and dissolution of igneous rocks with F-bearing minerals in the area (e.g., cryolite, biotite and amphiboles). Moderate to high correlations between Al and Fe ($r = 0.561$, $p < 0.01$), and Cd and Co ($r = 0.803$, $p < 0.01$), were attributed to similar geochemical processes and conditions for the release of these metals into the groundwater (Barzegar et al. 2015, 2016). Moderate correlation between Cl and Cd ($r = 0.630$, $p < 0.01$), and Cl and Co ($r = 0.500$, $p < 0.01$), suggested that these metals were released into groundwater by forming complexes in solution with evaporites (e.g., CdCl or CoCl) (Salminen et al. 2005; Soltani et al. 2017). Moderate correlations of As with Na ($r = 0.500$, $p < 0.01$), and As with K ($r = 0.552$, $p < 0.01$), possibly suggested a common geogenic origin of As and conditions that enhanced its mobility.

Cluster analysis (CA)

Based on the dendrogram produced by the HCA, groundwater samples were classified into two distinct clusters (Fig. 6a). Clusters 1 and 2 contained 80% and 20% of the total samples, respectively. Each cluster was divided into two sub-clusters (i.e., sub-clusters 1-1 and 1-2 for cluster 1 and sub-clusters 2-1 and 2-2 for cluster 2). Figure 6b shows the spatial distribution of the sub-clusters in the plain. To distinguish the important physicochemical parameters affecting the differences between sub-clusters, a one-way ANOVA was employed (Table 4). In this analysis, a significance value equal to zero showed a significant difference. There was a significant (sig. < 0.05) difference for all physicochemical parameters except Cr, Fe and Zn.

Box and whisker plots for the water quality variables were used to compare the sub-clusters (Fig. 7). According to the median values, pH and NO$_3$ concentrations were elevated and EC, Mg, Na, K, HCO$_3$, Cl, SO$_4$, SiO$_2$, Pb, Fe and As were lowest in sub-cluster 1-1 compared to the other sub-clusters. This sub-cluster was mainly located in the western and middle of the Khoy plain (Fig. 6b). The groundwater in these areas had a relatively low EC and high pH, which were mainly attributed to the recharge area in the west of the plain, to intensive agricultural activities and to the high coarse materials content of this part of the aquifer. Sub-cluster 1-2 had the lowest concentrations of NO$_3$ (attributed to the high fine materials content of this part of the aquifer) and Cr (attributed to the low impact of ultramafic and serpentinite rock), and was mainly situated in the east of the plain (Fig. 6b). Sub-cluster 2-1 had the highest As concentration, EC and dependent variables (i.e., Na, Cl, Mg), and was mainly located in the south of the plain, except for sample 5 in the northeast. These samples might be affected by the volcanic rocks, marl, sandstone, conglomerate and limestone in the southwest of the plain. Some parameters such as Ca, HCO$_3$, SO$_4$, F, SiO$_2$, Ni, Co, Pb, Cr, Al, Mn and Zn were elevated in sub-cluster 2-2. The samples of this sub-cluster were situated in the northern parts of the plain, and its characteristics could be attributed to the rocks
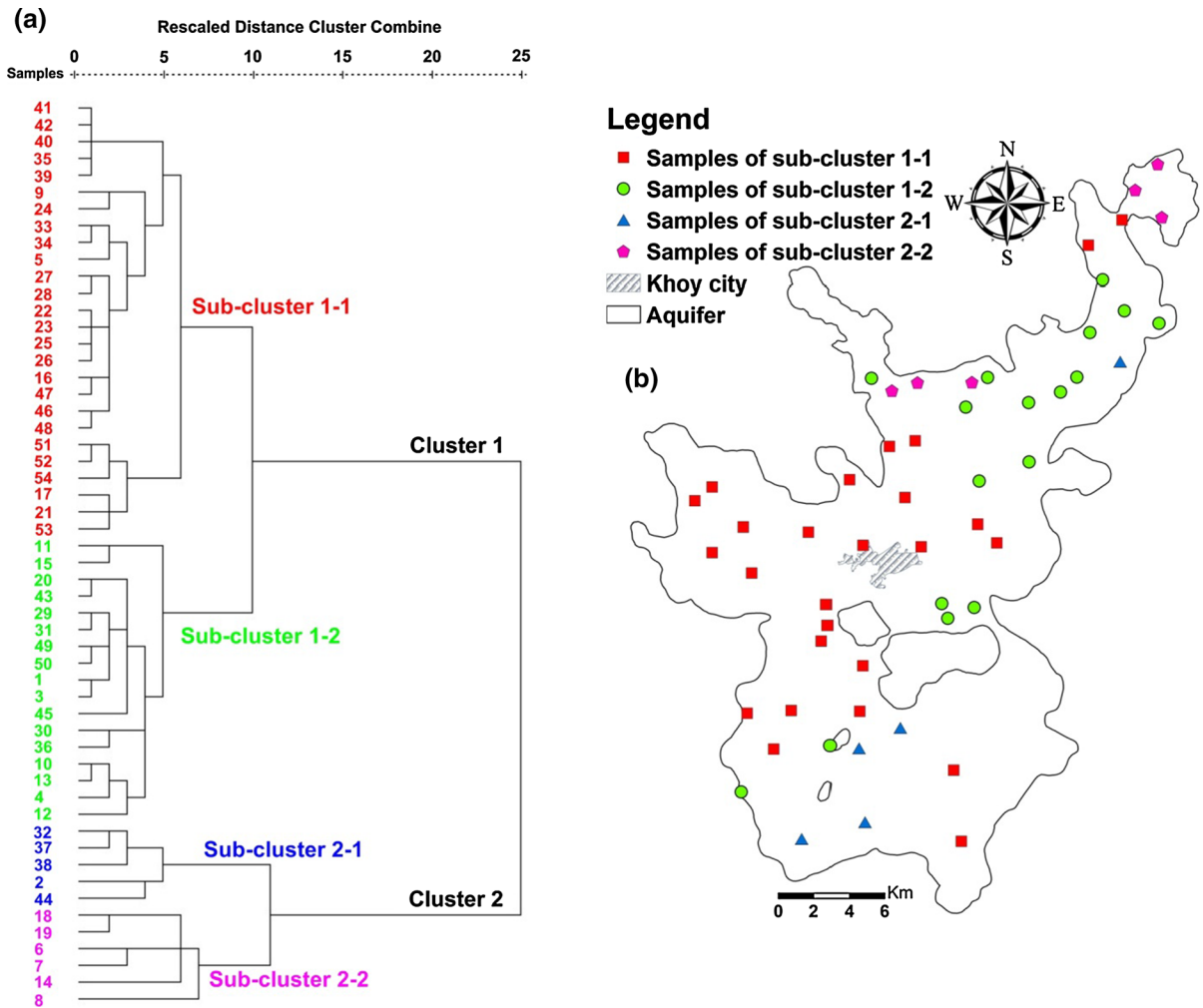
Fig. 6 **a** The dendrogram of groundwater samples for HCA; **b** spatial distribution of samples based on sub-clusters

in these areas (e.g., limestone, amphibolite, metamorphic and ultramafic rocks, serpentinite).

Factor analysis (FA)

The results of FA for physicochemical variables in the groundwater of the Khoy area are given in Table 5. The first factor accounted for 36.9% of the total variability (69.1%) and included EC, Na, K, Cl, SO_4, F and As parameters. This factor explained the effect of salinity on groundwater quality, which was due to weathering and dissolution of evaporitic minerals and also leaching of fertilizers from agricultural areas. Rowland et al. (2006) and Anawar et al. (2011) reported that As mainly occurs in the groundwater system in three phases including Fe and Mn oxides,

organic matter and silicate–sulfate. Although there was no strong correlation between As and other measured water quality parameters (there was a moderate correlation with Na and K), the presence of As and SO_4 indicated a silicate–sulfate phase as the possible source of As in the groundwater of the study area. As shown in Fig. 8a, FA1 contributed to the groundwater of the northeast and south of the plain where elevated values of EC were observed due to dissolution of the Miocene and Pliocene formations and evaporation occurring in shallow water tables.

The second factor with 13.2% of the total variance included pH, Ca, HCO_3, Pb and Mn. The presence of pH with negative strong loading indicated the effect of acidity on weathering and dissolution of the carbonate minerals and also in releasing Pb and Mn. This might

**Table 4** Results of the one-way ANOVA analysis between sub-clusters

Variable		Sum of squares	df^a	Mean square	F^b	Sig.^{c}
pH	Between sub-clusters	5.32	3	1.77	18.55	*0.0000*
	Within sub-clusters	4.78	50	0.10		
EC	Between sub-clusters	65,807,220.27	3	21,935,740.09	43.70	*0.0000*
	Within sub-clusters	25,098,005.23	50	501,960.10		
Ca	Between sub-clusters	609,100.10	3	203,033.37	44.84	*0.0000*
	Within sub-clusters	226,416.49	50	4528.33		
Mg	Between sub-clusters	23,015.96	3	7671.99	9.54	*0.0000*
	Within sub-clusters	40,197.26	50	803.95		
Na	Between sub-clusters	1,571,346.32	3	523,782.11	81.28	*0.0000*
	Within sub-clusters	322,225.87	50	6444.52		
K	Between sub-clusters	341.29	3	113.76	24.79	*0.0000*
	Within sub-clusters	229.46	50	4.59		
HCO_3	Between sub-clusters	3,634,392.55	3	1,211,464.18	28.76	*0.0000*
	Within sub-clusters	2,106,352.25	50	42,127.04		
Cl	Between sub-clusters	3,246,578.75	3	1,082,192.92	45.34	*0.0000*
	Within sub-clusters	1,193,348.09	50	23,866.96		
SO_4	Between sub-clusters	922,737.20	3	307,579.07	8.34	*0.0001*
	Within sub-clusters	1,843,833.47	50	36,876.67		
NO_3	Between sub-clusters	1655.66	3	551.89	4.82	*0.0050*
	Within sub-clusters	5724.13	50	114.48		
F	Between sub-clusters	1.45	3	0.48	8.39	*0.0001*
	Within sub-clusters	2.89	50	0.06		
SiO_2	Between sub-clusters	8837.17	3	2945.72	3.46	*0.0232*
	Within sub-clusters	42,629.62	50	852.59		
Ni	Between sub-clusters	160.76	3	53.59	64.42	*0.0000*
	Within sub-clusters	41.59	50	0.83		
Cd	Between sub-clusters	11.62	3	3.87	8.40	*0.0001*
	Within sub-clusters	23.05	50	0.46		
Co	Between sub-clusters	678.38	3	226.13	50.47	*0.0000*
	Within sub-clusters	224.00	50	4.48		
Pb	Between sub-clusters	224.50	3	74.83	4.74	*0.0055*
	Within sub-clusters	789.83	50	15.80		
Cr	Between sub-clusters	172.34	3	57.45	1.32	0.2784
	Within sub-clusters	2176.41	50	43.53		
Al	Between sub-clusters	9913.21	3	3304.40	3.52	*0.0215*
	Within sub-clusters	46,907.32	50	938.15		
Fe	Between sub-clusters	189,044.39	3	63,014.80	2.36	0.0822
	Within sub-clusters	1,332,835.15	50	26,656.70		
Mn	Between sub-clusters	2,714,318.36	3	904,772.79	29.30	*0.0000*
	Within sub-clusters	1,543,759.75	50	30,875.19		
Zn	Between sub-clusters	2613.76	3	871.25	1.50	0.2254
	Within sub-clusters	29,002.48	50	580.05		
As	Between sub-clusters	8103.99	3	2701.33	23.77	*0.0000*
	Within sub-clusters	5681.92	50	113.64		

The mean difference is significant at a level of 0.05. Italicized values are significant

[a] Degrees of freedom

[b] F-statistic

[c] Significance
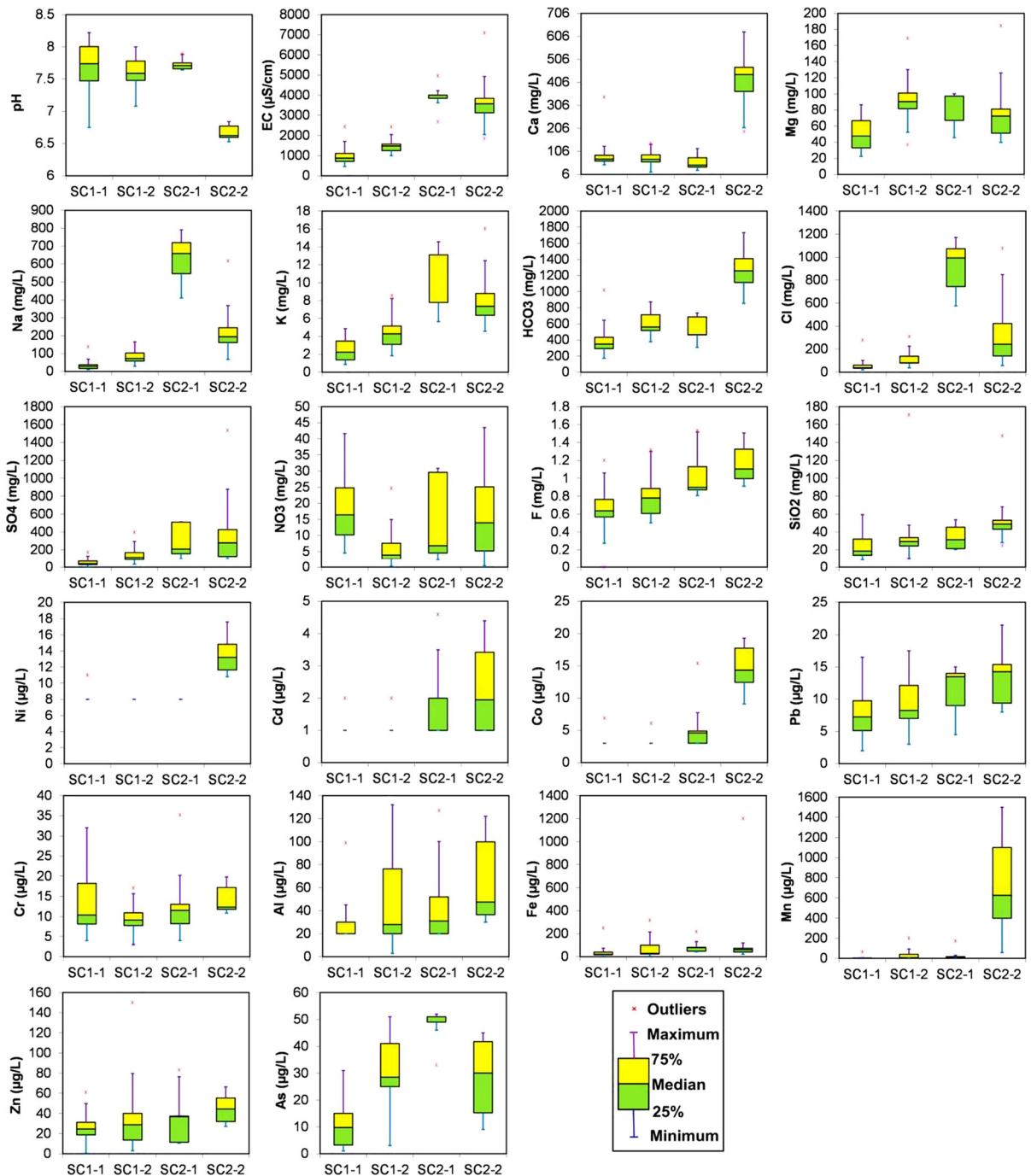
Fig. 7 Box and whisker plots of the water quality parameters in the cluster analysis

indicate the release of Mn from minerals including rhodochrosite ($MnCO_3$). Mn is partitioned into ferro-magnesian silicates and enriched in mafic and ultra-mafic rocks relative to felsic lithologies. Carbonate rocks, particularly dolostone, may also contain high

concentrations of Mn (Wedephol 1978), which can be deduced from the association between Mn and HCO_3. The spatial distribution of FA2 (Fig. 8b) confirmed that the northern parts of the aquifer were influenced by the weathering and dissolution of the formations.

Table 5 Factor loadings for the FA of the samples in the Khoy plain

Variable	FA1	FA2	FA3	FA4
pH	− 0.117	− 0.915	− 0.030	0.051
EC	0.837	0.454	0.113	0.228
Ca	0.228	0.815	0.080	0.311
Mg	0.415	0.066	0.329	0.500
Na	0.944	0.060	0.025	0.034
K	0.830	0.220	0.402	− 0.033
HCO_3	0.170	0.826	0.358	0.154
Cl	0.956	0.027	0.007	0.077
SO_4	0.699	0.350	− 0.087	0.442
NO_3	− 0.071	0.376	− 0.704	− 0.023
F	0.511	0.486	0.150	0.118
SiO_2	− 0.019	0.382	0.711	− 0.011
Pb	0.337	0.530	− 0.171	0.179
Cr	0.008	− 0.020	− 0.066	0.706
Al	0.319	0.145	0.660	0.177
Fe	− 0.017	0.344	0.686	0.038
Mn	0.035	0.679	0.287	− 0.222
Zn	0.113	0.101	0.125	0.575
As	0.512	− 0.005	0.460	− 0.416
% of variance	36.91	13.29	11.56	7.41
Cumulative %	36.91	50.21	61.77	69.18

FA3 had 11.5% of the total variance and included NO_3 with negative loading and SiO_2, Al and Fe with positive loadings, which possibly indicated the effect of both anthropogenic and natural processes on groundwater quality. The association between Mn and Fe could be attributed to the ready substitution of Mn with Fe in minerals. The occurrence of NO_3 with antithetic (negative) loading indicated anoxic conditions in the groundwater system (Anawar et al. 2003; Guo et al. 2011; Esmaeili et al. 2018) and also denitrification and nitrate reduction combined with other geochemical processes (Levins and Gosk, 2008; Usman et al. 2014). Mn and Fe are greatly influenced by redox conditions and easily mobilized as Mn^{2+} and Fe^{2+} under anoxic conditions (Hylander et al. 2000). In addition, agricultural activities and traffic might be a potential source for Mn in the groundwater. Geogenic sources of Fe and Mn are generally considered to be much more important than anthropogenic ones in the environment (Yang and Sanudo-Wilhelmy

1998), and the presence of SiO_2 may confirm the source as silicate minerals. Note that a single FA may interpret multiple processes, as reported previously (e.g., Arslan 2013; Kumaresan 2008; Yidana et al. 2010). The spatial distribution of FA3 is illustrated in Fig. 8c.

FA4 accounted for 7.4% of the total variance and included Mg, Cr and Zn with positive loadings. This factor was explained by weathering and dissolution of the mafic rocks including pyroxene, amphibole, serpentine and mica. Also, Zn is readily partitioned into silicate minerals by substitution with Mg, which has a similar ionic radius (Salminen et al. 2005). FA4 mainly covered the northern part of the plain in which igneous rocks are predominant (Fig. 8d).

Health risk assessment

The calculated HQ of trace elements to evaluate non-carcinogenic risk via ingestion for children and adults is given in Table 6. The order of HQ, according to the median values, was the same for both population groups:

As > Pb > Zn > Fe > Mn > Ni > Cu > Al > Cr.

Several similar studies have been carried out regarding the health risk assessment of multiple trace elements in the groundwater of Iran (e.g., Sakizadeh and Mirzaei 2016; Barzegar et al. 2018). In the study conducted by Barzegar et al. (2018), mean values of HQ indicated that As, with about a 95% contribution to the total non-carcinogenic risk and an HQ content greater than 1, was the most likely element in the groundwater of the Shabestar area, northwestern Iran, to induce a health risk in both population groups. HI values ranged between 0.49 and 11.33 (mean of 4.37) for children and between 0.21 and 4.85 (mean of 1.87) for adults. It was concluded that the dominant chronic risk level was high for children and low for adults. In Shush and Andimeshk, Khuzestan Province, southern Iran, Sakizadeh and Mirzaei (2016) reported the mean non-carcinogenic health risks for Cr, Cu and Mn were 0.62, 0.38 and 0.05, respectively. These results illustrated that as a whole the mean non-carcinogenic risk was below 1; however, Cu at ten stations (11% of total samples) and Cr at one station (1% of total samples) had HI values higher than 1. The lowest health risk was associated with Mn with a maximum HQ of 0.7, and the highest risk was from Cu with a HQ greater than 2.5 at some stations. In the current study,
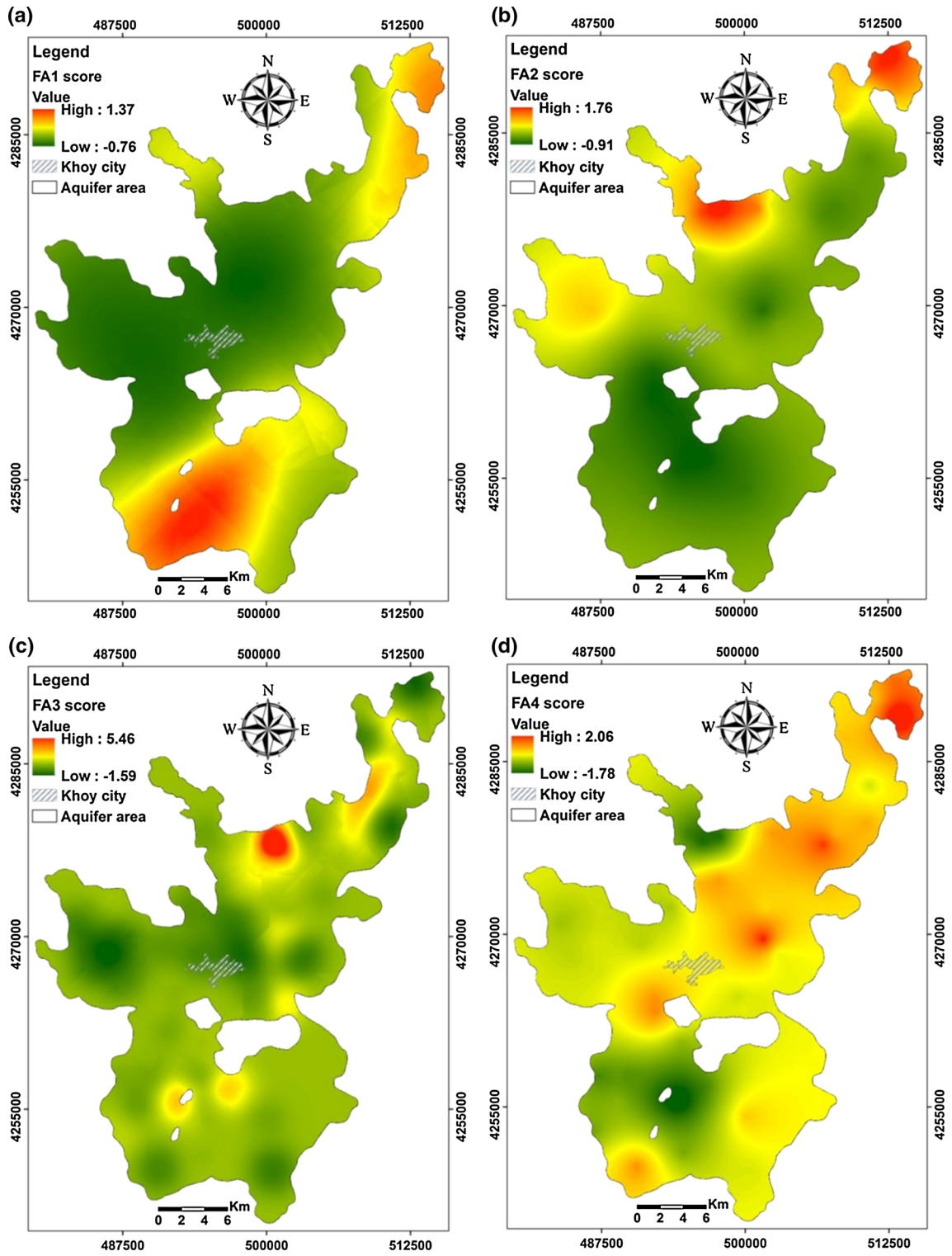
Fig. 8 Spatial distribution of factor scores for the FA

Table 6 Non-carcinogenic risk of trace elements in terms of hazard quotient (HQ) for children and adults in the Khoy area

| Trace element	HQ for children			HQ for adults		
	Minimum	Maximum	Median	Minimum	Maximum	Median
Ni	0.0267	0.0587	0.0267	0.0114	0.0251	0.0114
Cd	0.1333	0.6133	0.1333	0.0571	0.2629	0.0571
Co	0.6667	4.2889	0.6667	0.2857	1.8381	0.2857
Pb	0.0381	0.4095	0.1571	0.0163	0.1755	0.0673
Cr	0.0002	0.0016	0.0005	0.0001	0.0007	0.0002
Al	0.0013	0.0088	0.0015	0.0006	0.0038	0.0006
Fe	0.0013	0.1143	0.0031	0.0005	0.0490	0.0013
Mn	0.0014	2.1739	0.0064	0.0006	0.9317	0.0028
Zn	0.0001	0.0333	0.0063	0.0000	0.0143	0.0027
As	0.2222	11.5556	4.3333	0.0952	4.9524	1.8571

As and Cr were the elements with the maximum and minimum values of HQ, respectively, for children and adults, and had the highest and lowest impacts on the non-carcinogenic risk of groundwater in the area. The HQ for As exceeded the safe level (HQ = 1) for children ($HQ_{median} = 4.33$) and adults ($HQ_{median} = 1.85$), and HI ranged between 1.09 and 15.08 (mean of 4.37) for children, and from 0.46 to 6.46 (mean of 1.87), for adults. The HI for children for all samples was higher than one, which indicated that all samples were outside the acceptable range of non-carcinogenic risk. The minimum and maximum values of HI were 0.46 and 6.46 for samples 53 and 19, respectively, for the adult group, and were 1.09 and 15.08 for the same samples, respectively, for the children's group.

Comparison of the two aquifer types in the Khoy area (Fig. 9) showed that HQs of the unconfined aquifer samples were greater than those of the confined aquifer. The differences between the median HQs of aquifer samples for As (for adults: $HQ_{unconfined} = 2.23$ and $HQ_{confined} = 0.23$; for children:

$HQ_{unconfined} = 5.22$ and $HQ_{confined} = 0.55$) and Pb (for adults: $HQ_{unconfined} = 0.07$ and $HQ_{confined} = 0.02$; for children: $HQ_{unconfined} = 0.16$ and $HQ_{confined} = 0.04$) were significant. The differences between aquifer HQs for other elements (e.g., Ni, Cd, Co, Cr, Al, Fe, Mn and Zn) were not significant for either population group. The median HI values for the unconfined and confined aquifer samples were 2.89 and 0.62 for adults, and 6.74 and 1.46 for children, respectively. Therefore, the health risk associated with water consumption from the unconfined aquifer was higher than that from the confined aquifer in the study area.

The spatial distribution of HI values for children (Fig. 10a), according to the USEPA (1999) classification, showed that the samples with medium risk (30% of total samples) were mainly located in the west of the plain where the EC values of the groundwater were low. The samples with high risk (70% of total samples) for children were located in the northern and southern parts of the plain. The HI of samples for adults was classified into three levels of chronic risk, including

Fig. 9 HQ medians for unconfined and confined aquifers of the Khoy plain
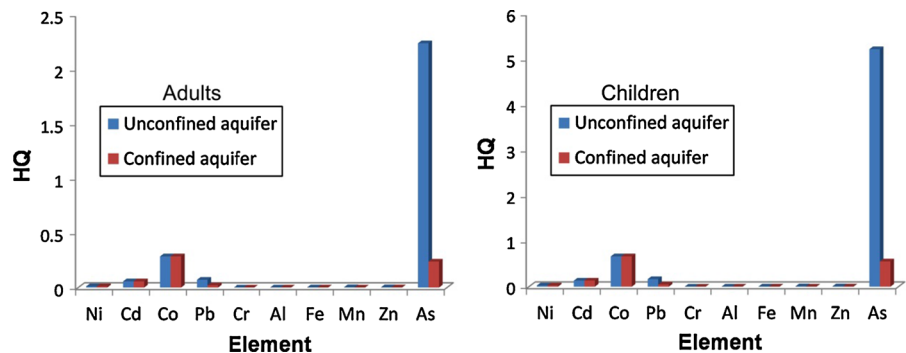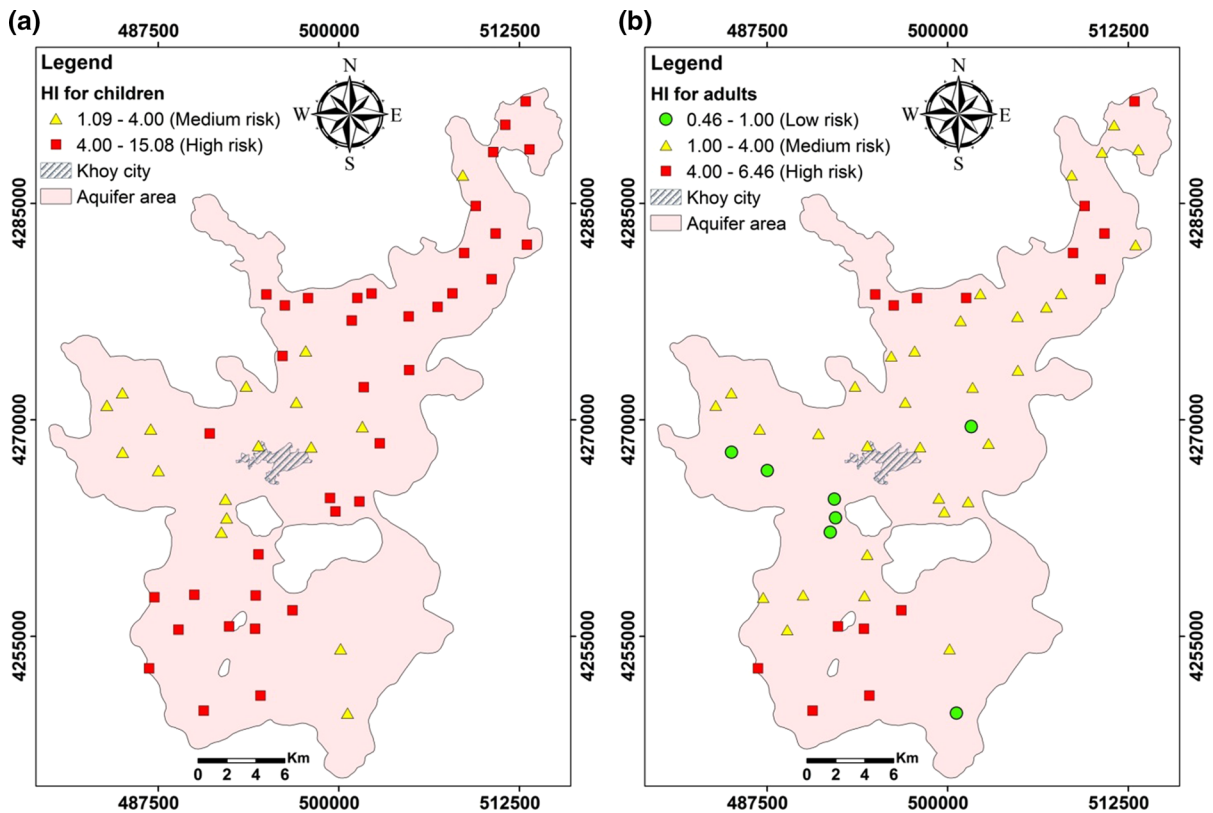
Fig. 10 Spatial distribution of hazard index (HI) values and the classification of samples based on non-carcinogenic risk **a** for children and **b** for adults

low (34% of samples), medium (16% of samples) and high (45% of samples) according to the USEPA (1999) classification. The spatial distribution of the HI for adults (Fig. 10b) illustrated that high-risk samples were mainly situated in the north and south of the plain.

The health risk assessment outcomes showed that people living in the Khoy area who were exposed to trace metals through drinking water had a non-carcinogenic risk. Therefore, a permanent monitoring and remediation of trace elements (particularly As) in groundwater of the area is crucial.

Conclusions

Water quality parameters measured in 54 water samples from the Khoy plain in northwestern Iran showed that EC values and its major dependent ions (except K) were above the permissible levels for drinking according to the USEPA (1999). Moreover,

the concentrations of some trace elements (i.e., Pb, Zn, Cd and As) exceeded the permissible levels for drinking and could affect the health of the local people.

Multivariate analysis, including correlation, cluster and factor analyses, showed the contribution of both natural and anthropogenic factors to groundwater quality in the area. Based on the cluster analysis (CA), water samples were categorized into two distinct clusters and each cluster included two sub-clusters. The ANOVA statistical procedure revealed that all of the physicochemical parameters except Cr, Fe and Zn affected the difference between sub-clusters. Sub-cluster 1-1 samples in the western and middle of the plain had elevated concentrations of pH and NO_3 and the lowest levels of EC, Mg, Na, K, HCO_3, Cl, SO_4, SiO_2, Pb, Fe and As compared to other sub-clusters. Sub-cluster 2-1 samples in the southern part of the plain contained elevated values of As, EC and its dependent variables (i.e., Na, Cl, Mg). The quality of

samples in the sub-clusters was mainly affected by the geological units around sample locations.

Factor analysis (FA) indicated that the quality of groundwater in the Khoy area was mainly controlled by geogenic factors. Salinity was the major cause of deterioration of water quality in the area, which may be attributed to the weathering and dissolution of evaporitic minerals from Miocene and Pliocene units and leaching of fertilizers from agricultural areas. It can be concluded that an acidic environment may have resulted in the release of some trace elements (e.g., Pb, Mn, Ni and Co) into groundwater in the area. Redox conditions were another possible factor resulting in the release of Fe and Mn into the groundwater from silicate minerals, which was justified by negative loadings of NO_3 in FA3. The presence of Cr and Zn was attributed to mafic rocks including pyroxene, amphibole, serpentine and mica in which Zn is readily partitioned into silicate minerals by substitution of Mg.

Based on chronic health risk assessment results, Cr and As had the lowest and highest impacts on the non-carcinogenic risk of groundwater in the area with hazard quotient values of 0.0001 and 11.55, respectively. The health risk associated with consumption of unconfined aquifer water was higher than that of confined aquifer water in the area. The high-risk samples for both children and adults were mainly situated in the northeast and southwest of the plain where the groundwater was saline. Decision makers should pay attention to groundwater management in these areas where over-exploitation of groundwater may cause elevated salinity and redox conditions, which could generate aquifer conditions that would further release trace elements into the groundwater.

References

Adriano, D. C. (2001). *Trace elements in terrestrial environments: Biogeochemistry, bioavailability, and risks of metals* (2nd ed.). New York: Springer.

Anawar, H. M., Akai, J., & Sakugaqa, H. (2003). Mobilization of arsenic from subsurface sediments by the effect of bicarbonate ions in groundwater. *Chemosphere*, *54*, 753–762.

Anawar, H. M., Akai, J., Mihaljevič, M., Sikder, A. M., Ahmed, G., Tareq, S. M., et al. (2011). Arsenic contamination in groundwater of Bangladesh: Perspectives on geochemical, microbial and anthropogenic issues. *Water, 3,* 1050–1076. https://doi.org/10.3390/w3041050.

Arslan, H. (2013). Application of multivariate statistical techniques in the assessment of groundwater quality in seawater intrusion area in Bafra Plain, Turkey. *Environmental Monitoring and Assessment, 185,* 2439–2452.

Balkhair, K. S., & Ashraf, M. A. (2016). Field accumulation risks of heavy metals in soil and vegetable crop irrigated with sewage water in western region of Saudi Arabia. *Saudi Journal of Biological Sciences, 23*(1), 32–44.

Barzegar, R., Asghari Moghaddam, A., & Kazemian, N. (2015). Assessment of heavy metals concentrations with emphasis on arsenic in the Tabriz plain aquifers, Iran. *Environmental Earth Sciences, 74*(1), 297–313.

Barzegar, R., Asghari Moghaddam, A., Soltani, S., Fijani, E., Tziritis, E., & Kazemian, N. (2018). Heavy metal(loid)s in the groundwater of Shabestar area (NW Iran): Source identification and health risk assessment. *Exposure and Health.* https://doi.org/10.1007/s12403-017-0267-5.

Barzegar, R., Asghari Moghaddam, A., & Tziritis, E. (2016). Assessing the hydrochemistry and water quality of the Aji-Chay River, northwest of Iran. *Environmental Earth Sciences, 75*(23), 1486.

Barzegar, R., Asghari Moghaddam, A., Tziritis, E., Fakhri, M. S., & Soltani, S. (2017). Identification of hydrogeochemical processes and pollution sources of groundwater resources in the Marand plain, northwest of Iran. *Environmental Earth Sciences, 76*(7), 297.

Belzile, N., Chen, Y. W., Gunn, J. M., & Dixit, S. S. (2004). Sediment trace metal profiles in lakes of Killarney Park, Canada: From regional to continental influence. *Environmental Pollution, 130*(2), 239–248.

Bhuiyan, M., Rakib, M. A., Dampare, S. B., Ganyaglo, S., & Suzuki, S. (2011). Surface water quality assessment in the central part of Bangladesh using multivariate analysis. *KSCE Journal of Civil Engineering, 15*(6), 995–1003.

Bingöl, D., Ay, Ü., Bozbaş, S. K., & Uzgören, N. (2013). Chemometric evaluation of the heavy metals distribution in waters from the Dilovası region in Kocaeli, Turkey. *Marine Pollution Bulletin, 68*(1–2), 134–139.

Bortey-Sam, N., Nakayama, S. M., Ikenaka, Y., Akoto, O., Baidoo, E., Mizukawa, H., et al. (2015). Health risk assessment of heavy metals and metalloid in drinking water from communities near gold mines in Tarkwa, Ghana. *Environmental Monitoring and Assessment, 187*(7), 397.

Celebi, A., Sengour, B., & Klove, B. (2014). Human health risk assessment of dissolved metals in groundwater and surface waters in the Melen watershed, Turkey. *Journal of Environmental Science and Health, Part A: Toxic/Hazardous Substances & Environmental Engineering, 49,* 153–161.

Domenico, P. A., & Schwartz, F. W. (1998). *Physical and chemical hydrogeology* (2nd ed., p. 506). New York: John Wiley.

Duggal, V., Rani, A., Mehra, R., & Balaram, V. (2017). Risk assessment of metals from groundwater in northeast Rajasthan. *Journal of Geological Society of India, 90*(1), 77–84.

El Alfy, M., Lashin, A., Abdalla, F., & Al-Bassam, A. (2017). Assessing the hydrogeochemical processes affecting groundwater pollution in arid areas using an integration of geochemical equilibrium and multivariate statistical techniques. *Environmental Pollution, 229,* 760–770. https://doi.org/10.1016/j.envpol.2017.05.052.

Esmaeili, S., Asghari Moghaddam, A., Barzegar, R., & Tziritis, E. (2018). Multivariate statistics and hydrogeochemical modeling for source identification of major elements and heavy metals in the groundwater of Qareh-Ziaeddin plain, NW Iran. *Arabian Journal of Geosciences, 11,* 5.

Giri, S., & Singh, A. K. (2015). Human health risk assessment via drinking water pathway due to metal contamination in the groundwater of Subarnarekha River Basin, India. *Environmental Monitoring and Assessment, 187,* 63–76.

Guo, H., Zhang, B., Li, Y., Berner, Z., Tang, X., Norra, S., et al. (2011). Hydrogeological and biogeochemical constrains of arsenic mobilization in shallow aquifers from the Hetao basin, Inner Mongolia. *Environmental Pollution, 159*(4), 876–883.

Hardle, W., & Simar, L. (2007). *Applied multivariate statistical analysis* (2nd ed.). Berlin: Springer.

Hylander, L. D., Meili, M., Oliveira, L. J., Silva, E. D. E., Guimaraes, J. R. D., Araujo, D. M., et al. (2000). Relationship of mercury with aluminum, iron and manganese oxy-hydroxides in sediments from the Alto Pantanal, Brazil. *The Science of the Total Environment, 260,* 97–107.

IBM Corp. (2012). *IBM SPSS statistics for windows, version 21.0.* Armonk, NY: IBM Corp.

Järup, L. (2003). Hazards of heavy metal contamination. *British Medical Bulletin, 68,* 167–182.

Kaiser, H. F. (1960). The application of electronic computers to factor analysis. *Educational and Psychological Measurement, 20,* 141–151.

Kumaresan, P. R. M. (2008). Factor analysis and linear regression model (LRM) of metal speciation and physicochemical characters of groundwater samples. *Environmental Monitoring and Assessment, 138,* 65–79.

Levins, I., & Gosk, G. (2008). Trace elements in groundwater as indicators of anthropogenic impact. *Environmental Geology, 55,* 285–290.

Li, P., Li, X., Meng, X., Li, M., & Zhang, Y. (2016). Appraising groundwater quality and health risks from contamination in a semiarid region of northwest China. *Exposure and Health, 8*(3), 361–379. https://doi.org/10.1007/s12403-016-0205-y.

Li, P., & Qian, H. (2011). Human health risk assessment for chemical pollutants in drinking water source in Shizuishan City, Northwest China. *Iranian Journal of Environmental Health Science and Engineering, 8*(1), 41–48.

Li, P., Qian, H., Howard, K. W. F., & Wu, J. (2015). Heavy metal contamination of Yellow River alluvial sediments, northwest China. *Environmental Earth Sciences, 73*(7), 3403–3415. https://doi.org/10.1007/s12665-014-3628-4.

Li, P., Tian, R., Xue, C., & Wu, J. (2017). Progress, opportunities and key fields for groundwater quality research under the impacts of human activities in China with a special focus on western China. *Environmental Science and Pollution Research, 24*(15), 13224–13234. https://doi.org/10.1007/s11356-017-8753-7.

Li, P., Wu, J., Qian, H., Lyu, X., & Liu, H. (2014). Origin and assessment of groundwater pollution and associated health risk: A case study in an industrial park, northwest China. *Environmental Geochemistry and Health, 36*(4), 693–712. https://doi.org/10.1007/s10653-013-9590-3.

Liang, C. P., Wang, S. W., Kao, Y. H., & Chen, J. S. (2016). Health risk assessment of groundwater arsenic pollution in southern Taiwan. *Environmental Geochemistry and Health, 38,* 1271–1281.

Ma, H. W., Hung, M. L., & Chen, P. C. (2007). A systemic health risk assessment for the chromium cycle in Taiwan. *Environment International, 33*(2), 206–218.

Nabavi, M. H. (1976). *An introduction to the geology of Iran* (p. 109). Tehran: Geological Survey of Iran. **(in Persian)**.

Nguyen, V. A., Bang, S., Viet, P. H., & Kim, K. W. (2009). Contamination of groundwater and risk assessment for arsenic exposure in Ha Nam Province, Vietnam. *Environment International, 35*(3), 466–472.

Otto, M. (1998). Multivariate methods. In R. Kellner, J. M. Mermet, M. Otto, & H. M. Widmer (Eds.), *Analytical chemistry* (p. 916). Weinheim: WileyVCH.

Piper, A. M. (1944). A graphic procedure in the geochemical interpretation of water analyses. *Transactions American Geophysical Union, 25,* 914–928.

Prüss-Ustün, A., Vickers, C., Haefliger, P., & Bertollini, R. (2011). Knowns and unknowns on burden of disease due to chemicals: A systematic review. *Environmental Health, 10,* 9.

Purushothaman, P., Rao, M. S., Rawat, Y. S., Kumar, C. P., Krishan, G., & Parveen, T. (2014). Evaluation of hydrogeochemistry and water quality in Bist-doab region, Punjab, India. *Environmental Earth Sciences, 72*(3), 693–706.

Radfar, H., Amini, B., Khalaatbari, M., Emami, M. H., & Bahremand, M. (2005). *Geological map of Khoy sheet (1:100,000).* Tehran: Geological Survey of Iran.

Rahman, M. M., Ng, J. C., & Naidu, R. (2009). Chronic exposure of arsenic via drinking water and its adverse health impacts on humans. *Environmental Geochemistry and Health, 31,* 189–200.

Rowland, H. A. L., Polya, D. A., Lloyd, J. R., & Pancost, R. D. (2006). Characterisation of organic matter in a shallow, reducing, arsenicrich aquifer, West Bengal. *Organic Geochemistry, 37,* 1101–1114.

Sakizadeh, M., & Mirzaei, R. (2016). Health risk assessment of Fe, Mn, Cu, Cr in drinking water in some wells and springs of Shush and Andimeshk, Khuzestan Province, Southern Iran. *Iranian Journal of Toxicology, 10*(2), 29–35.

Salminen, R., Batista, M. J., Bidovec, M., Demetriades, A., De Vivo, B., De Vos, W., Duris, M., Gilucis, A., Gregorauskiene, V., Halamic, J., Heitzmann, P., Lima, A., Jordan, G., Klaver, G., Klein, P., Lis, J., Locutura, J., Marsina, K., Mazreku, A., O'Connor, P. J., Olsson, S., Ottesen, R. T., Petersell, V., Plant, J. A., Reeder, S., Salpeteur, I., Sandström, H., Siewers, U., Steenfeldt, A., & Tarvainen, T. (2005). *FOREGS geochemical atlas of Europe, part 1: Background information, methodology and maps.* Geological Survey of Finland, Espoo, p 525, 36 figures, 362 maps.

Singh, H., Singh, D., Singh, S. K., & Shukla, D. N. (2017). Assessment of river water quality and ecological diversity through multivariate statistical techniques, and earth observation dataset of rivers Ghaghara and Gandak, India. *International Journal of River Basin Management*, *15*(3), 347–360.

Soltani, S., Asghari Moghaddam, A., Barzegar, R., Kazemian, N., & Tziritis, E. (2017). Hydrogeochemistry and water quality of the Kordkandi-Duzduzan plain, NW Iran: Application of multivariate statistical analysis and PoS index. *Environmental Monitoring and Assessment, 189*(9), 455.

Srivastava, S. K., & Ramanathan, A. L. (2008). Geochemical assessment of groundwater quality in vicinity of Bhalswa landfill, Delhi, India, using graphical and multivariate statistical methods. *Environmental Geology, 53*(7), 1509–1528.

Su, H., Kang, W., Xu, Y., & Wang, J. (2017). Assessing groundwater quality and health risks of nitrogen pollution in the Shenfu mining area of Shaanxi Province, Northwest China. *Exposure and Health*. https://doi.org/10.1007/s12403-017-0247-9.

Sun, L., Peng, W., & Cheng, C. (2016). Source estimating of heavy metals in shallow groundwater based on UNMIX. Model: A case study. *Indian Journal of Geo-Marine Sciences, 45*(6), 756–762.

Tziritis, E., Datta, P. S., & Barzegar, R. (2017). Characterization and assessment of groundwater resources in a complex hydrological basin of central Greece (Kopaida basin) with the joint use of hydrogeochemical analysis, multivariate statistics and stable isotopes. *Aquatic Geochemistry, 23*(4), 271–298.

Tziritis, E., Skordas, K., & Kelepertsis, A. (2016). The use of hydrogeochemical analyses and multivariate statistics for the characterization of groundwater resources in a complex aquifer system. A case study in Amyros River basin, Thessaly, central Greece. *Environmental Earth Sciences, 75*(4), 1–11.

U.S. Environmental Protection Agency. (1999). *A risk assessment multi-way exposure spreadsheet calculation tool*. Washington, DC: United States Environmental Protection Agency.

Usman, U. N., Toriman, M. E., Juahir, H., Abdullahi, M. G., Rabiu, A. A., & Isiyaka, H. (2014). Assessment of groundwater quality using multivariate statistical techniques in Terengganu. *Science and Technology, 4*(3), 42–49. https://doi.org/10.5923/j.scit.20140403.02.

Ward, J. H. (1963). Hierarchical grouping to optimize an objective function. *Journal of the American Statistical Association, 301,* 236–244.

Wedepohl, K. H. (1978). Manganese. In K. H. Wedepohl (Ed.), *Handbook of geochemistry* (Vol. 11/3, pp. 25-K-1/25-K-17). Berlin: Springer.

Wongsasuluk, P., Chotpantarat, S., Siriwong, W., & Robson, M. G. (2014). Heavy metal contamination and human health risk assessment in drinking water from shallow groundwater wells in an agricultural area in Ubon Ratchathani Province, Thailand. *Environmental Geochemistry and Health, 36,* 169–182.

World Health Organization. (2011). *Guidance for immunotoxicity risk assessment for chemicals*. IPCS harmonization project document; no. 10, Geneva.

Wu, J., Li, P., Qian, H., Duan, Z., & Zhang, X. (2014). Using correlation and multivariate statistical analysis to identify hydrogeochemical processes affecting the major ion chemistry of waters: Case study in Laoheba phosphorite mine in Sichuan, China. *Arabian Journal of Geosciences, 7*(10), 3973–3982. https://doi.org/10.1007/s12517-013-1057-4.

Wu, J., & Sun, Z. (2016). Evaluation of shallow groundwater contamination and associated human health risk in an alluvial plain impacted by agricultural and industrial activities, mid-west China. *Expo Health, 8*(3), 311–329. https://doi.org/10.1007/s12403-015-0170-x.

Wu, M. L., Wang, Y. S., Su, C. C., Wang, H., Dong, J. D., Yin, J. P., et al. (2010). Identification of coastal water quality by statistical analysis methods in Daya Bay, South China Sea. *Marine Pollution Bulletin, 60*(6), 852–860.

Yang, M., & Sanudo-Wilhelmy, S. (1998). Cadmium and manganese distribution in the Hudson River estuary: Interannual and seasonal variability. *Earth and Planetary Science Letters, 19,* 982–992.

Yeganeh, J., Nazemi, S., & Yousefzadeh, A. (2015). Assessment of the effect of human and industrial activities on groundwater within the city of Khoy. *International Journal of Health Studies, 1*(2), 26–33. https://doi.org/10.22100/ijhs.v1i2.59.

Yidana, S. M., Yakubo, B. B., & Akabzaa, T. M. (2010). Analysis of groundwater quality using multivariate and spatial analyses in the Keta basin, Ghana. *Journal of African Earth Sciences, 58,* 220–234.

Zhang, Y., Wu, J., & Xu, B. (2018). Human health risk assessment of groundwater nitrogen pollution in Jinghui canal irrigation area of the loess region, northwest China. *Environmental Earth Sciences, 77*(7), 273. https://doi.org/10.1007/s12665-018-7456-9.